Vol. 130: 109–115, 2018
https://doi.org/10.3354/dao03267

DISEASES OF AQUATIC ORGANISMS
Dis Aquat Org

Published September 10

Red seabream iridovirus associated with cultured Florida pompano *Trachinotus carolinus* mortality in Central America

Adrian Lopez-Porras[1], Juan A. Morales[1], Gilbert Alvarado[2], Samantha A. Koda[3], Alvin Camus[4], Kuttichantran Subramaniam[3], Thomas B. Waltzek[3], Esteban Soto[5,*]

[1]Servicio de Patologia Veterinaria, Universidad Nacional de Costa Rica, Heredia, Costa Rica
[2]Laboratory of Experimental and Comparative Pathology (LAPECOM), Biology School, University of Costa Rica, Costa Rica
[3]Department of Infectious Diseases and Immunology, College of Veterinary Medicine, University of Florida, Gainesville, Florida 32611, USA
[4]Department of Pathology, College of Veterinary Medicine, University of Georgia, Athens, Georgia 30602, USA
[5]Department of Medicine and Epidemiology, University of California, School of Veterinary Medicine, Davis, California 95616, USA

ABSTRACT: Mariculture of Florida pompano *Trachinotus carolinus* in Central America has increased over the last few decades and it is now a highly valued food fish. High feed costs and infectious diseases are significant impediments to the expansion of mariculture. Members of the genus *Megalocytivirus* (MCV), subfamily *Alphairidovirinae*, within the family *Iridoviridae*, are emerging pathogens that negatively impact Asian mariculture. A significant mortality event in Florida pompano fingerlings cultured in Central America occurred in October 2014. Affected fish presented with abdominal distension, darkening of the skin, and periocular hemorrhages. Microscopic lesions included cytomegalic 'inclusion body-bearing cells' characterized by basophilic granular cytoplasmic inclusions in multiple organs. Transmission electron microscopy revealed arrays of hexagonal virions (155–180 nm in diameter) with electron-dense cores within the cytoplasm of cytomegalic cells. Pathological findings were suggestive of an MCV infection, and the diagnosis was later confirmed by partial PCR amplification and sequencing of the viral gene encoding the myristylated membrane protein. The viral sequence revealed that the fingerlings were infected with an MCV genotype, red seabream iridovirus (RSIV), previously reported only from epizootics in Asian mariculture. This case underscores the threat RSIV poses to global mariculture, including the production of Florida pompano in Central America.

KEY WORDS: Florida pompano · *Trachinotus carolinus* · Red seabream iridovirus · RSIV · *Megalocytivirus* · Inclusion body-bearing cells

INTRODUCTION

Aquaculture is one of the world's fastest developing food production sectors. The industry has experienced rapid growth in recent years as global catches from wild fisheries have plateaued or declined since the 1980s (Worm et al. 2009, FAO 2016a). Global production of cultured fish, crustaceans, and mollusks rose from 1×10^6 t in 1950 to 73.8×10^6 t in 2014 (FAO 2016a). Aquaculture is soon predicted to produce the majority of fish consumed by humans, and intensive aquaculture production systems are expected to surpass any growth in global wild fisheries in the near future (Cressey 2009, Klinger & Naylor 2012, FAO

*Corresponding author: sotomartinez@ucdavis.edu

2016a). Mariculture of *Trachinotus* spp. has been particularly attractive due to the high economic value of the snubnose pompano *T. blochii* in Asia-Pacific and Florida pompano *T. carolinus* in the Americas (FAO 2016b).

Viral diseases pose one of the most significant threats to the aquaculture industry (Walker & Winton 2010). The growth of aquaculture, along with the increased international movement of fish and fish products, has facilitated the emergence and rapid dissemination of several potentially devastating infectious disease agents. Notable among these are members of the genus *Megalocytivirus* (MCV) within the subfamily *Alphairidovirinae,* family *Iridoviridae* (Chinchar et al. 2017). Megalocytiviruses are globally emerging pathogens resulting in significant mortalities in cultured ornamental and food fish stocks (Chinchar 2002, Shinmoto et al. 2009, Subramaniam et al. 2012). Infectious spleen and kidney necrosis virus (ISKNV) is the type species in the genus MCV and includes genotypes such as the red seabream iridovirus (RSIV), which is associated with disease in >30 marine fish species cultured throughout Asia (Chinchar et al. 2009, Jancovich et al. 2012, Waltzek et al. 2012, Kawato et al. 2017, OIE 2018). The major capsid protein, ATPase, and myristylated membrane protein genes have been used to differentiate closely related MCV genotypes, including 2 closely related clades of the RSIV genotype (Go et al. 2016, Koda et al. 2018). RSIV disease (RSIVD) caused by either the RSIV or ISKNV genotypes, is notifiable to the World Organisation for Animal Health (OIE) (Kawakami & Nakajima 2002, Kawato et al. 2017, OIE 2018).

Histologically, MCV infections are characterized by the presence of cytomegalic 'inclusion body-bearing cells' (IBCs). Immature IBCs resemble blast cells, with abundant, foamy, pale, basophilic cytoplasm and enlarged, central, round nuclei containing a prominent nucleolus (Mahardika et al. 2004, Miyazaki 2007). Darker staining, mature inclusions often occupy the entire cell cytoplasm, compressing the nucleus against the cell membrane. These IBCs have been described as amoeba-like, hypertrophic cells, heteromorphic balloon cells, and circumscribed bodies (Armstrong & Ferguson 1989, Inouye et al. 1992, Anderson et al. 1993, Chua et al. 1994, Sudthongkong et al. 2002). In this study, histopathology, transmission electron microscopy (TEM), and end-point PCR were used to diagnose RSIV infection associated with a high mortality disease outbreak in cultured Florida pompano fingerlings in the Caribbean Sea.

MATERIALS AND METHODS

Clinical history

In October 2014, a fish mariculture farm located in the Caribbean Sea, Central America, experienced high mortality in net-pen-reared Florida pompano fingerlings over a period of several weeks. Gross findings in moribund fish, as reported by the farmer, included coelomic distension, darkening, lethargy, increased respiratory rate, exophthalmia, and periocular hemorrhages. Formalin-fixed samples of skin, gills, heart, liver, spleen, stomach, intestines, pancreas, and ovaries from 5 pompano fingerlings were submitted to the Department of Pathology, School of Veterinary Medicine, Universidad Nacional de Costa Rica, for microscopic examination.

Histopathology

Formalin-fixed tissues from 5 fingerlings were processed routinely for histological examination. Three to 5 samples of each submitted tissue type were embedded in paraffin, sectioned at 5 µm, and stained with hematoxylin and eosin (H&E) and Giemsa stains for light microscopic examination.

TEM

Cardiac tissue from a paraffin block was selected for TEM evaluation at the Centro de Investigación en Estructuras Microscópicas (CIEMIC), University of Costa Rica, San Jose, Costa Rica. The paraffin-embedded tissue was deparaffinized in 100% xylene, rehydrated, and processed for TEM using a standard protocol (Hayat 1989). Ultrathin sections (60 nm) were post-stained with 2% uranyl acetate followed by lead citrate and examined using a Hitachi HT7700 electron microscope.

DNA extraction, PCR amplification, sequencing, and BLASTN analysis

Three 5 µm sections were cut from a block containing spleen and heart tissues. The tissues were deparaffinized and DNA extracted using a Qiagen DNA formalin-fixed, paraffin-embedded (FFPE) Tissue Kit following the manufacturer's instructions. The extracted DNA was subjected to a partially validated pan-MCV conventional PCR assay designed specifi-

cally to amplify MCVs from FFPE samples (Koda et al. 2018). The primers (MCV-F; 5′-CAA CCC CAC GTC CAA AGA-3′ and MCV-R; 5′-ACA TTG CTG GGG CAT GTG-3′) amplify 173 bp (including the primer sequences) of the MCV gene encoding the myristylated membrane protein. A negative water control and a positive control (MCV-positive Nile tilapia *Oreochromis niloticus* sample; Subramaniam et al. 2016) were also used in the PCR for quality control. Reaction volumes for the pan-MCV PCR were 50 l and consisted of 0.25 µl of Platinum *Taq* DNA Polymerase (Invitrogen), 5.0 µl of 10× PCR Buffer, 2.0 µl of 50 mM $MgCl_2$, 1.0 µl of 10 mM dNTPs, 2.5 µl of 20 µM forward and reverse primers, 32.25 µl of molecular grade water, and 4.5 µl of DNA template. An initial denaturation step of 95°C for 5 min was followed by 40 cycles of a 94°C denaturation step, a 55°C annealing step, and a 72°C extension step, each step run for 30 s, and a final extension step at 72°C for 5 min (Koda et al. 2018). The PCR product was visualized on a 1% agarose gel stained with ethidium bromide. A PCR purification kit (Qiagen) was used to purify amplicons that were sequenced on an ABI 3130 platform (Applied Biosystems). A BLASTN search of the resulting sequence against the National Center for Biotechnology Information (NCBI) non-redundant (nr) nucleotide database (www.ncbi.nlm.nih.gov/blast/Blast.cgi) was employed to confirm the suspected MCV infection and determine the particular MCV genotype as previously described (Koda et al. 2018).

RESULTS

Histopathology

The greatest number of IBCs were observed in the ventricular myocardium of the heart. Trabeculae were markedly expanded and distorted by IBCs, most abundant in the spongy layer adjacent to the compact myocardium (Fig. 1A). Pale-staining, immature IBCs outnumbered mature IBCs in the sections examined. Small numbers of mononuclear inflammatory cells infiltrated the endocardium, myocardium, pericardium, and bulbus arteriosus in association with large numbers of IBCs, which were best visualized with the Giemsa stain (Fig. 1B).

Numerous IBCs were widely distributed in the spleen, most commonly in periarteriolar macrophage sheaths (ellipsoids). Clusters of IBCs were accompanied by perivascular inflammation, vasculitis, hemorrhage, and scattered necrotic cellular debris (Fig. 2A). In the liver, small numbers of IBCs were observed primarily in the sub-endothelium of portal veins, central veins, and sinusoids, in association with mild mononuclear inflammatory cell infiltrates (Fig. 2B). Immature and mature IBCs accompanied by similar vascular and perivascular inflammatory changes were also present in the exocrine pancreas, as well as the gastrointestinal lamina propria, muscularis, and serosa (Fig. 2C). Moderate numbers of IBCs were present in branchial lamellae. The filamental

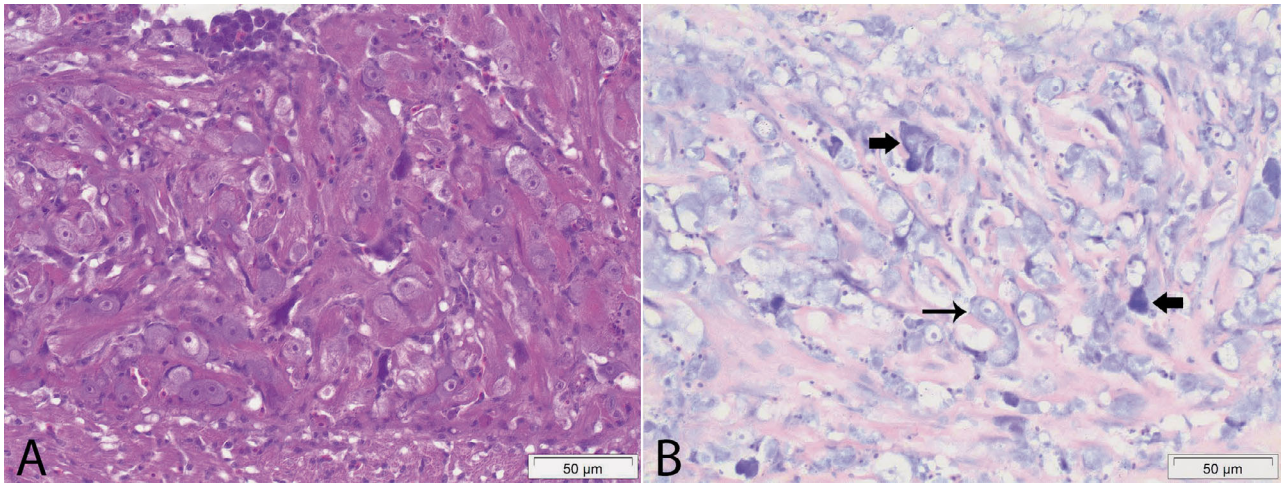

Fig. 1. Histologic sections of heart from a Florida pompano *Trachinotus carolinus* fingerling infected with red seabream iridovirus. (A) Ventricular myocardium at the junction of the spongy and compact layers. The subendothelium of the spongy layer contains large numbers of predominantly immature blast-like inclusion body-bearing cells (IBCs) that obscure the normal mesh-like architecture of the tissue. H&E stain. (B) IBCs were best visualized with Giemsa staining. Immature inclusions have pale staining, finely granular to foamy cytoplasm, and enlarged nuclei with prominent nucleoli (thin arrow). Mature IBCs appear more irregular and have darker staining homogeneous cytoplasm. Peripheralized nuclei are frequently masked by the inclusion (thick arrows)

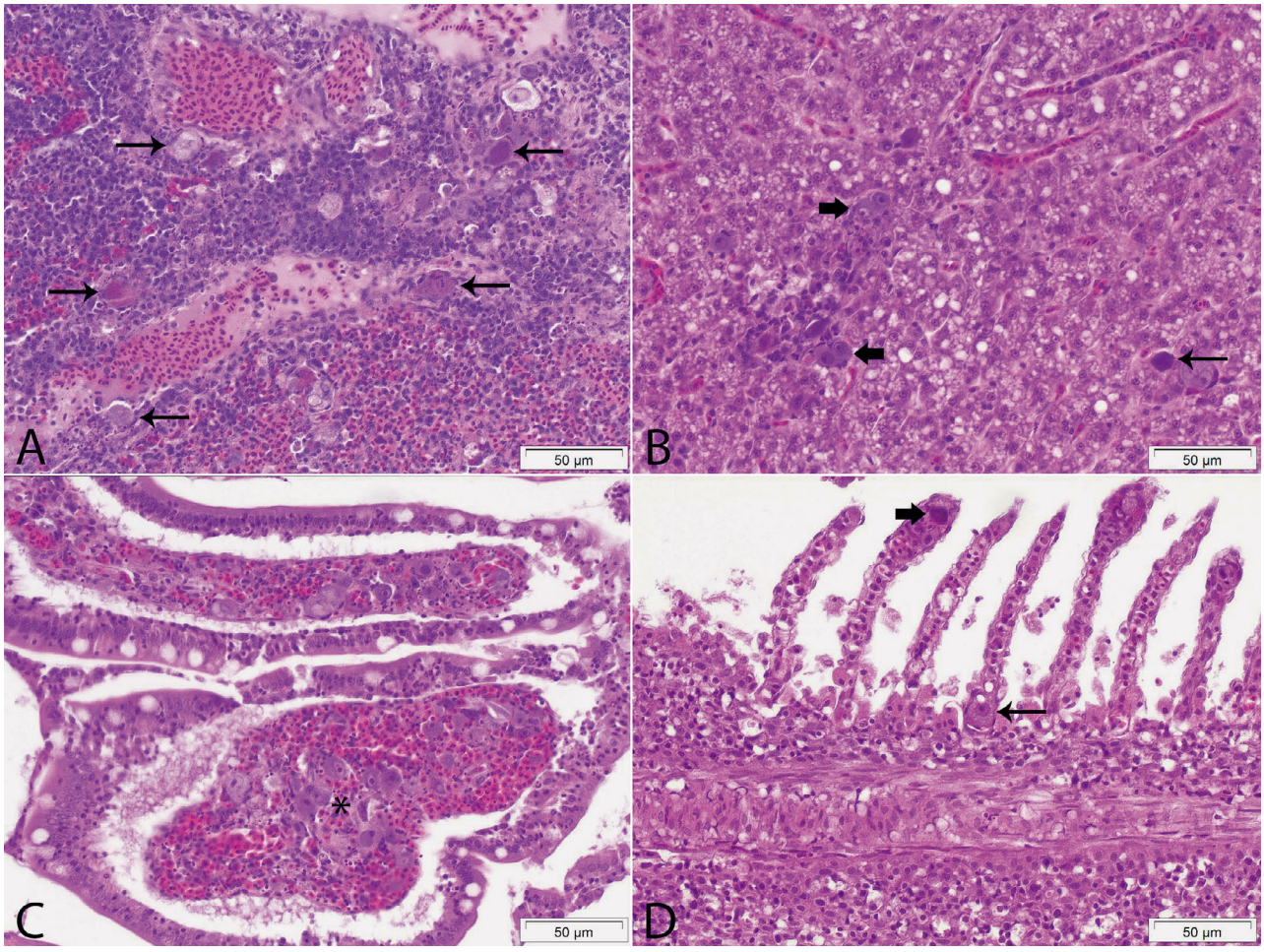

Fig. 2. Histologic sections (H&E stain) of multiple tissues from a Florida pompano *Trachinotus carolinus* fingerling demonstrating red seabream iridovirus inclusion body-bearing cells (IBCs). (A) Spleen. IBCs (arrows) were numerous and associated primarily with ellipsoids, resulting in vasculitis and perivascular necrosis. (B) Liver. IBCs were scattered in the parenchyma adjacent to sinusoids (thin arrow) and more commonly in the subendothelium of larger vessels (thick arrows) accompanied by mild mononuclear inflammation. (C) Intestine. The gastrointestinal lamina propria was congested, hemorrhagic, and contained numerous IBCs (asterisk). The mucosa was microscopically normal. (D) Gill. The filamental epithelium is infiltrated by small numbers of mononuclear cells. An immature IBC is located in the subepithelium of a lamellar base (thin arrow) and a mature IBC is present in a lamellar tip (thick arrow)

epithelium was infiltrated by small numbers of mononuclear inflammatory cells (Fig. 2D). The ovarian connective tissue stroma and capsule also contained small numbers of IBCs, primarily in perivascular locations (Fig. 3). These findings were consistent across all 5 fish processed.

TEM

Numerous viral particles were readily observed in the cytoplasm of IBCs within cardiac tissue (Miyazaki 2007). The cytoplasmic hexagonal viral nucleocapsids were unenveloped and formed paracrystalline arrays. Nucleocapsids measured between 155 and 180 nm in diameter and had a central electron-dense core with a diameter of 85 nm (Fig. 4), as previously described for MCVs (Jancovich et. al. 2012).

Sequencing and BLASTN analysis

The PCR yielded the expected 173 bp band (Fig. 5). After removal of the primer sequences, the BLASTN analysis revealed highest nucleotide sequence identity (100%) to RSIV strain Ehime-1 (GenBank accession no. AB104413, Kurita et al. 2002), an RSIV Clade 1 MCV (Go et al. 2016, Koda et al. 2018).

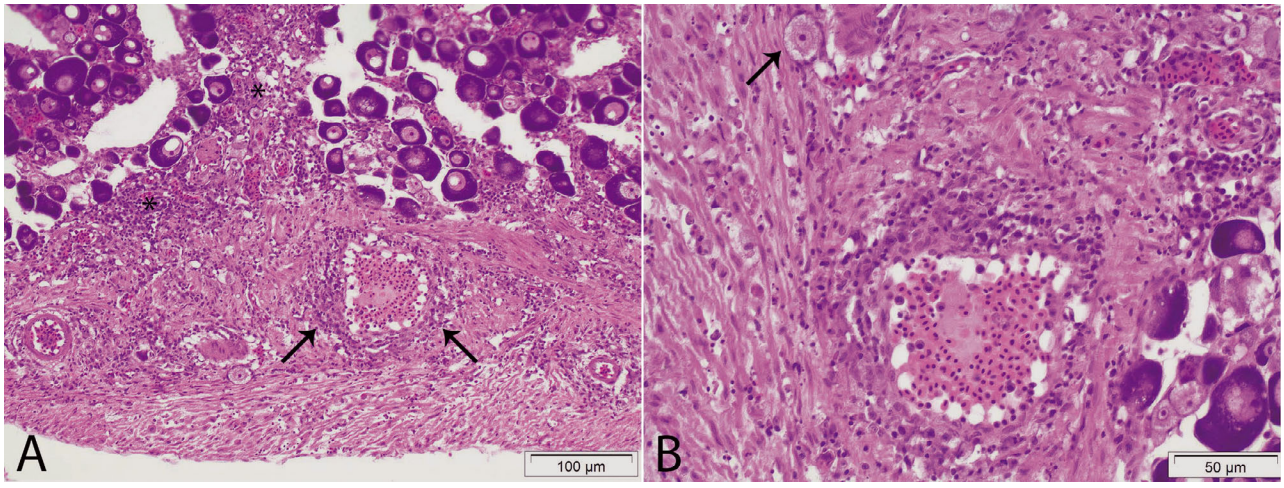

Fig. 3. Ovary from a Florida pompano *Trachinotus carolinus* fingerling infected with red seabream iridovirus. (A) Perivascular (arrows) and stromal (asterisks) mononuclear inflammation. (B) Immature, blast-like inclusion body-bearing cells (arrow) were scattered within the ovarian stroma and connective tissue capsule

DISCUSSION

Reports of viral diseases affecting cultured snubnose pompano include betanodavirus (Ransangan et al. 2011) and RSIV (OIE 2018). Microscopic examination of the diseased fingerlings in our study revealed widespread megalocytes with prominent cytoplasmic inclusions often located adjacent to vascular lumens. The observed IBCs and ultrastructural features of the associated viral particles are characteristic of MCV infections (Sudthongkong et al. 2002, Gibson-Kueh et al. 2003, Mahardika et al. 2008, Weber et al. 2009). PCR amplification and sequencing of the partial gene sequence encoding the myristylated membrane protein confirmed that the outbreak was due to a Clade 1 RSIV MCV (Go et al. 2016, Koda et al. 2018). In addition to the pan-MCV assay, we also tested the sample against the OIE conventional PCR primer set RSIV1 (Kurita et al. 1998) which targets a *Pst*I restriction fragment and has an amplicon size of 570 bp. However, the results of the OIE primer set were negative for this sample. It is important to note that the OIE primer set is not currently validated for FFPE tissues. Furthermore, the large amplicon size of the OIE primer set is not ideal for FFPE tissue samples that often contain degraded DNA due to fixation. This likely explains why the OIE primer set was negative and the pan-MCV primer set designed to amplify

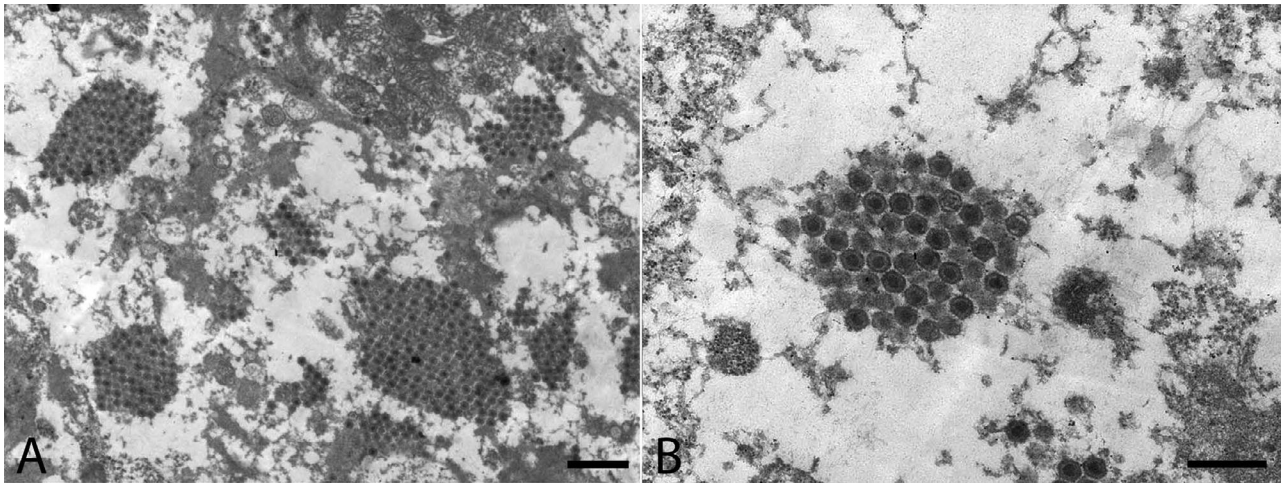

Fig. 4. Transmission electron microscopic findings in cultured Florida pompano *Trachinotus carolinus* fingerling infected with red seabream iridovirus. (A) Myocardial inclusion body-bearing cells with paracyrstalline arrays of viral particles. Scale bar = 1 µm. (B) Higher magnification of (A), revealing hexagonal-shaped nucleocapsids with dense central cores. Scale bar = 1 µm

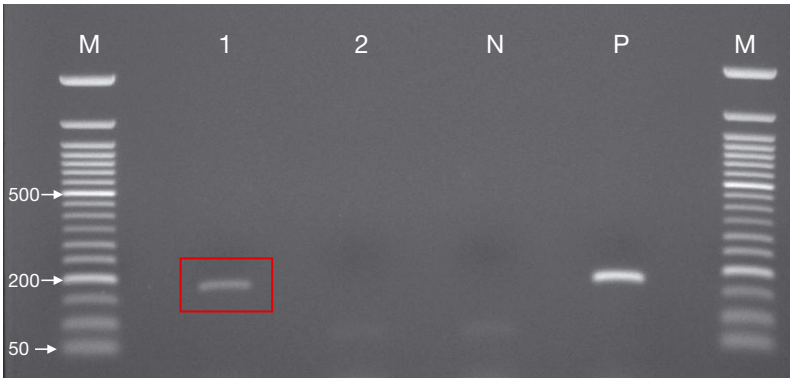

Fig. 5. PCR product (173 bp, red box) amplified by using MCV-F and MCV-R primers. M: 50 base pair ladder; Lane 1: Florida pompano *Trachinotus carolinus* fingerling formalin-fixed, paraffin-embedded (FFPE) tissue DNA sample; Lane 2: no-template negative control (extraction); N: no-template negative control (water); P: ISKNV-infected Nile tilapia *Oreochromis niloticus* FFPE tissue DNA positive control (Subramaniam et al. 2016). The 50, 200, and 500 bp marks on the ladder are indicated by arrows

MCVs in FFPE tissue sample was positive (Koda et al. 2018). Historically limited to Asian mariculture operations (Song et al. 2008, Kurita & Nakajima 2012), this case confirms findings by Koda et al. (2018) that the distribution of RSIV is expanding beyond Asia and now poses a threat to American aquaculture.

The occurrence of this OIE-reportable pathogen in Caribbean mariculture warrants future monitoring and research. Clinical signs and gross lesions associated with this case, including coelomic distension, darkening, lethargy, increased respiratory rate, exophthalmia, hemorrhage, and splenomegaly, suggested an infectious etiology but were non-specific. Microscopically, MCV infections are typified by the presence of characteristic IBCs that are typically most numerous in the spleen, where necrosis can be extensive. However, IBCs can occur in most tissues, particularly renal hematopoietic tissue and glomeruli, the endocardium, branchial central venous sinuses and filamental subepithelium, gastrointestinal lamina propria and serosa, connective tissues, and rarely the central nervous system. In this study, the greatest number of IBCs were observed in the ventricular myocardium of the heart. IBCs are often associated with or protrude into vascular lumens, but necrosis is usually limited outside the spleen as observed in our study. Parenchymal cells and skin and mucosal epithelial cells are not affected (Gibson-Kueh et al. 2003). The precise cell type(s) developing inclusions is uncertain. The association of IBCs with perivascular locations and connective tissues suggests that fibroblasts may be involved, but hematopoietic cells may also be targeted (Gibson-Kueh et al. 2003, Weber et al. 2009, Kawato et al. 2017).

MCVs are of particular concern due to their lack of host specificity. Epidemics in Japan occur annually in the same area, spreading horizontally at temperatures above 20°C, often between adjacent net pens. The existence of a carrier state remains uncertain, but survivors become resistant and may serve as a source of infection to newly introduced naïve fish (Kawato et al. 2017). RSIVD has not been reported in hatcheries, implying that vertical transmission is unlikely (Nakajima & Kurita 2005, Yanong & Waltzek 2013). However, the presence of IBCs in the ovaries of diseased pompano and other fish species (Gibson-Kueh et al. 2003) suggests that vertical transmission may be possible and should be studied further. Diagnostic confirmation is usually made by PCR of infected tissue DNA (OIE 2018) and/or detection of viral antigen or DNA by indirect immunofluorescent antibody tests (Nakajima et al. 1995) and *in situ* hybridization protocols, respectively (Chao et al. 2004, Weber et al. 2009, Go et al. 2016). While there are no specific treatments for RSIVD, a formalin-killed vaccine is currently available in Japan for vaccinating red sea bream *Pagrus major*, striped jack *Pseudocaranx dentex*, Malabar grouper *Epinephelus malabaricus*, orange-spotted grouper *E. coioides*, and other fish species in the genus *Seriola* (OIE 2018).

Acknowledgements. We acknowledge assistance from Laura Alvarado (Servicio de Patologia Veterinaria, Universidad Nacional de Costa Rica) in preparation of sections for DNA extraction and routine histology. We also thank Dr. Denise Imai (Comparative Pathology Laboratory at the University of California, Davis) for critical review of the manuscript. This study was partially funded by FOCAES-UNA.

LITERATURE CITED

Anderson IG, Prior HC, Rodwell BJ, Harris GO (1993) Iridovirus-like virions in imported dwarf gourami (*Colisa lalia*) with systemic amoebiasis. Aust Vet J 70:66–67

Armstrong RD, Ferguson HW (1989) Systemic viral disease of the chromide cichlid *Etroplus maculatus.* Dis Aquat Org 7:155–157

Chao CB, Chen CY, Lai YY, Lin CS, Huang HT (2004) Histological, ultrastructural, and *in situ* hybridization study on enlarged cells in grouper *Epinephelus* hybrids infected by grouper iridovirus in Taiwan (TGIV). Dis Aquat Org 58:127–142

Chinchar VG (2002) Ranaviruses (family *Iridoviridae*): emerging cold-blooded killers. Arch Virol 147:447–470

Chinchar VG, Hyatt A, Miyazaki T, Williams T (2009) Family *Iridoviridae*: poor viral relations no longer. Curr Top Microbiol Immunol 328:123–170

Chinchar VG, Hick P, Ince IA, Jancovich JK and others (2017) ICTV virus taxonomy profile: *Iridoviridae.* J Gen Virol 98:890–891

Chua FHC, Ng ML, Ng KL, Loo JJ, Wee JY (1994) Investigation of outbreaks of a novel disease, 'Sleepy Grouper Disease', affecting the brown-spotted grouper, *Epinephelus tauvina* Forskal. J Fish Dis 17:417–427

Cressey D (2009) Future fish. Nature 458:398–400

FAO (Food and Agriculture Organization of the United Nations) (2016a) The state of the world fisheries and aquaculture 2016. FAO, Rome

FAO (2016b) Cultured aquatic species information programme — *Trachinotus* spp. FAO Fisheries and Aquaculture Department, FAO, Rome

Gibson-Kueh S, Netto P, Ngoh-Lim GH, Chang SF and others (2003) The pathology of systemic iridoviral disease in fish. J Comp Pathol 129:111–119

Go J, Waltzek TB, Subramaniam K, Yun SC and others (2016) Detection of infectious spleen and kidney necrosis virus (ISKNV) and turbot reddish body iridovirus (TRBIV) from archival ornamental fish samples. Dis Aquat Org 122:105–123

Hayat MA (1989) Principles and techniques of electron microscopy: biological applications. CRC Press, Boca Raton, FL

Inouye K, Yamano K, Maeno Y, Nakajima K, Matsuoka M, Wada Y, Sorimachi M (1992) Iridovirus infection of cultured red sea bream, *Pagrus major.* Fish Pathol 27:19–27

Jancovich JK, Chinchar VG, Hyatt A, Miyazaki T, Williams T, Zhang QY (2012) Family *Iridoviridae.* In: King AMQ, Adams MJ, Carstens EB, Lefkowitz EJ (eds) Virus taxonomy: ninth report of the International Committee on Taxonomy of Viruses. Elsevier Academic Press, San Diego, CA, p 193–210

Kawakami H, Nakajima K (2002) Cultured fish species affected by red sea bream iridoviral disease from 1996 to 2000. Fish Pathol 37:45–47

Kawato Y, Subramaniam K, Nakajima K, Waltzek TB, Whittington R (2017) Iridoviral diseases: red sea bream iridovirus and white sturgeon virus. In Woo PTK, Cipriano RC (eds) Fish viruses and bacteria: pathobiology and protection. Elsevier Academic Press, San Diego, CA, p 147–159

Klinger D, Naylor R (2012) Searching for solutions in aquaculture: charting a sustainable course. Annu Rev Environ Resour 37:247–276

Koda SA, Subramaniam K, Francis-Floyd R, Yanong RP and others (2018) Phylogenomic characterization of two novel members of the genus *Megalocytivirus* from archived ornamental fish samples. Dis Aquat Org 130:11–24

Kurita J, Nakajima K (2012) Megalocytiviruses. Viruses 4: 521–538

Kurita J, Nakajima K, Hirono I, Aoki T (1998) Polymerase chain reaction (PCR) amplification of DNA of red sea bream iridovirus (RSIV). Fish Pathol 33:17–23

Kurita J, Nakajima K, Hirono I, Aoki T (2002) Complete genome sequencing of Red Sea Bream Iridovirus (RSIV). Fish Sci 68(Suppl II):1113–1115

Mahardika K, Zafran, Yamamoto A, Miyazaki T (2004) Susceptibility of juvenile humpback grouper *Cromileptes altivelis* to grouper sleepy disease iridovirus (GSDIV). Dis Aquat Org 59:1–9

Mahardika K, Haryanti, Muzaki A, Miyazaki T (2008) Histopathological and ultrastructural features of enlarged cells of humpback grouper *Cromileptes altivelis* challenged with Megalocytivirus (family Iridoviridae) after vaccination. Dis Aquat Org 79:163–168

Miyazaki T (2007) Colour atlas of fish histopathology, Vol 2. ShinSuisan Shinbun-Sha, Tokyo

Nakajima K, Kurita J (2005) Red sea bream iridoviral disease. Uirusu 55:115–125

Nakajima K, Maeno Y, Fukodome M, Fukuda Y, Tanaka S, Matsuoka S, Sorimachi M (1995) Immunofluorescence test for the rapid diagnosis of red seabream iridovirus infection using monoclonal antibody. Fish Pathol 30: 115–119

OIE (World Organisation for Animal Health) (2018) Red Sea bream iridoviral disease. In: Manual of diagnostic tests for aquatic animals. www.oie.int/index.php?id=2439&L=0&htmfile=chapitre_rsbid.htm (accessed 10 Feb 2018)

Ransangan J, Manin BO, Abdullah A, Roli Z, Sharudin E (2011) Betanodavirus infection in golden pompano, *Trachinotus blochii*, fingerlings cultured in deep-sea cage culture facility in Langkawi, Malaysia. Aquaculture 315: 327–334

Shinmoto H, Taniguchi K, Ikawa T, Kawai K, Oshimaet S (2009) Phenotypic diversity of infectious red sea bream iridovirus isolates from cultured fish in Japan. Appl Environ Microbiol 75:3535–3541

Song JY, Kitamura SI, Jung SJ, Miyadai T and others (2008) Genetic variation and geographic distribution of megalocytiviruses. J Microbiol 46:29–33

Subramaniam K, Shariff M, Omar AR, Hair-Bejo M (2012) Megalocytivirus infection in fish. Rev Aquacult 4:221–233

Subramaniam K, Gotesman M, Smith CE, Steckler NK, Kelley KL, Groff JM, Waltzek TB (2016) Megalocytivirus infection in cultured Nile tilapia *Oreochromis niloticus*. Dis Aquat Org 119:253–258

Sudthongkong C, Miyata M, Miyazaki T (2002) Iridovirus disease in two ornamental tropical freshwater fishes: African lampeye and dwarf gourami. Dis Aquat Org 48: 163–173

Walker PJ, Winton JR (2010) Emerging viral diseases of fish and shrimp. Vet Res 41:51

Waltzek TB, Marty GD, Alfaro ME, Bennett WR and others (2012) Systemic iridovirus from threespine stickleback *Gasterosteus aculeatus* represents a new megalocytivirus species (family *Iridoviridae*). Dis Aquat Org 98: 41–56

Weber ES III, Waltzek TB, Young DA, Twitchell EL and others (2009) Systemic iridovirus infection in the Banggai cardinalfish (*Pterapogon kauderni* Koumans 1933). J Vet Diagn Invest 21:306–320

Worm B, Hilborn R, Baum JK, Branch TA and others (2009) Rebuilding global fisheries. Science 325:578–585

Yanong RPE, Waltzek TB (2013) Megalocytivirus infections in fish, with emphasis on ornamental species. UF/IFAS Extension FA182. University of Florida, Gainesville, FL

Editorial responsibility: James Jancovich, San Marcos, California, USA

Submitted: February 14, 2018; Accepted: June 29, 2018
Proofs received from author(s): August 16, 2018